Cooperative control strategy for an airplane landing on a mobile target

Rogelio Lozano, Armando Alatorre, Pedro Castillo Garcia

Noname manuscript No.
(will be inserted by the editor)

Cooperative control strategy for an airplane landing on a mobile target

Rogelio Lozano*, **Armando Alatorre, Pedro Castillo**

Received: date / Accepted: date

Abstract This paper presents a cooperative control strategy for landing a fixed-wing drone on a mobile target vehicle. The control strategy focuses on guiding the drone along a desired trajectory while the target vehicle's speed is controlled so that both reach the desired position simultaneously. The system model is composed by the kinematic model of a fixed-wing drone and a ground vehicle. A state feedback control based on Lie derivatives is determined applying the input-output analysis. The system stability is obtained by using Lyapunov stability theory. The proposed control strategy is evaluated in numerical simulations to validate its performance.

Keywords Dynamic path following, landing nonlinear control, fixed-wing drone, Lie derivatives, target tracking.

1 INTRODUCTION

In recent years, due to their low-cost, the use of fixed-wing unmanned aerial vehicles has increased. Flying at high altitudes, long distances, and high speeds are the main advantages of these vehicles. In addition, the fixed-wing vehicles' main applications are photogrammetry, agriculture activities, ground vehicle tracking, search, rescue, and package delivery.

Once the Unmanned Aerial Vehicle (UAV) has completed its mission, the next flight operation is landing.

R. Lozano, P. Castillo & A. Alatorre are with Université de technologie de Compiègne, CNRS, Heudiasyc (Heuristics and Diagnosis of Complex Systems), CS 60319 - 60203 Compiègne Cedex, France. Emails: (rlozano, castillo, aalatorr)@hds.utc.fr. R. Lozano & A. Alatorre are also with the Center of Research and Advanced Studies of the National Polytechnic Institute (CINVESTAV).

Landing is a critical stage since the UAV must execute it with precision. However, some factors such as wind disturbances and pilot inexperience can affect the maneuver and lead to accidents [1].

Therefore, the research community has focused on automatic landing to avoid damages to the vehicle structure. The automatic landing for a fixed-wing drone on a runway is divided in three phases: descending flight, flare maneuver, and taxiing such that is described in [2]. An automatic landing is not an easy task, thus some vision algorithms support aircraft control such as the alignment to the runway [3] or the estimation of the position and speed with respect to a target [4].

In [5], a flight maneuver is proposed for an automatic landing at a specific coordinate. The authors design a strategy to lead the aircraft in deep stall conditions to a specific point with the least airspeed. In [6], the authors propose the recovery of a fixed-wing vehicle using a vision algorithm to identify an air dome. They developed a recovery test, the drone navigates towards the dome's position, which is mounted on a moving car.

We consider the challenge of landing on a moving vehicle, which is relevant and useful for the UAVs. For specific tasks, some fixed-wing drones require to be light. In [7], the authors propose to eliminate the need for landing gear by using a mobile ground vehicle landing strategy. A cooperative control is considered with the restriction that the speed and position of both vehicles will converge at the same time. The above strategy was improved in [8], the authors design a cooperative control for a rendezvous point at a finite distance, using a Model Predictive Control (MPC). However, Lyapunov stability analysis is not presented.

Inspired by this project, we focus on studying Dynamic Path Following (DPF). DPF consists of steering an autonomous vehicle towards a trajectory, which is

defined by the movement of a target. In the literature, an autonomous vehicle is defined as the target where all its states can be known by the follower, [9, 10].

This strategy is commonly used to monitor and track vehicles. In [9], the authors develop a strategy for a fixed-wing drone to follow a reference circular trajectory, which is focused on a moving ground vehicle. The dynamic path following approach has been studied by the authors, taking into account the movement of the target in both two and three dimensions as presented in [10] and [11]. Moreover, the use of multiple vehicles to follow a trajectory, and to deal with the coordination problems is studied in [12].

As is mentioned in [13], the control algorithms for dynamic path following impose the convergence of the follower vehicle towards a desired trajectory parametrized by the path length of the target vehicle. The second task is to control the evolution of the path parameter dynamics, i.e., the target speed.

Some DPF control algorithms are focused on the tracking error constraints [14], the vehicle parameter uncertainty [15] and to attenuate external disturbances, as in [16]. The authors develop a DPF strategy using underwater vehicles. They propose a robust controller of first-order sliding mode and a disturbance observer where the external disturbances are defined as the maritime currents. The same approach was used for a fixed-wing drone in [17], the authors propose a control based on a nonlinear observer to deal with the wind disturbance, which is estimated and involved in the path following control law, improving the system performance.

Another applied strategy to reach or keep a distance to the target position is the rendezvous guidance control. This approach is focused on the alignment and speed regulation with respect to the target. In [18], the authors develop a recovery system of a drone. The goal is to guide the drone towards the funnel of a mothership-cable-drogue system, which is moving. Similar work is developed in [19], the authors develop a guidance strategy of a mothership vehicle for keeping the drogue in a circular trajectory, and the follower aircraft rendezvous with the drogue using a vision algorithm.

Much of the research about rendezvous uses the guidance geometry method. This method focuses on the angular difference between the moving target and the follower [20]. In [21], the authors propose to apply this guidance control method for a fixed-wing drone, which rendezvous to a reference point that moves in a circular path. Besides, differential geometry is commonly used to guide missiles to intercept mobile targets, as in [22].

Complex applications are proposed such as path planning for multiple fixed-wing drones developing a simultaneous rendezvous on a target in an environment with obstacles [23, 24]. In [25], the authors increase the challenge of the above tasks, considering the arrival time towards one or multiple targets. The strategy can be applied to the pursuit of intruder vehicles.

Another application concerns a fixed-wing vehicle which will rendezvous with an autonomous vehicle for refueling. In [26], the authors propose a guidance law to align the tanker aircraft with respect to the velocity vector of the receiver aircraft, keeping constraints while in flight. In [27], the UAV refueling process is carried out by an unmanned ground vehicle (UGV), which is used as a mobile refueling unit. An optimal control law is designed to guide the UAV towards a desired altitude, keeping the same velocity as the UGV.

Comparing the research works found on the literature to carry out the convergence of a fixed-wing drone towards the position of a target vehicle, the rendezvous approach with a control based on differential geometry is a method more complex than the dynamic path following since the last method can be addressed to a problem of trajectory tracking. Considering the MPC methodology, the design of this kind of controller is a difficult task for a cooperative approach because it is necessary to define a discrete model of the system with certain state constraints of both vehicles. These models are solved by iterative algorithms, obtaining the optimal values of the control inputs in each sample time. The developer must be careful with the computational cost when processing the optimal solution since it could generate delays. This affects the performance of the vehicles and fail to land. In comparison, our cooperative control strategy is easy to implement and the vehicles reach the desired landing position simultaneously.

In this work, we propose a control strategy to guide a fixed-wing drone towards a moving ground vehicle. The system model is defined by their kinematic equations, such as in [28]. A control strategy will be developed to stabilize the lateral motion of the target vehicle and the aerial vehicle.

The first goal is to align the target vehicle to the X axis, and the aircraft to the $X-Z$ plane where the coordinate system related to the inertial frame is denoted by $\{I\}$. The alignment strategy is illustrated in Figure 1, the red circle represents the ground vehicle (x_g, y_g) and the gray circle depicts the fixed-wing vehicle (x, y). Once both vehicles are aligned the kinematic equations are simplified. Therefore, we can focus on the longitudinal system, which tends to be an underactuated system since it has two control inputs and five state variables. The path parameter is defined as the target position x_g. Moreover, we propose a descending flight trajectory to reach the target.

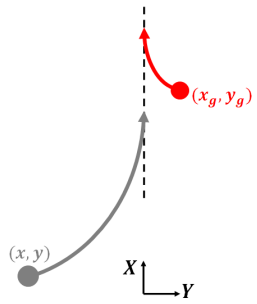

Fig. 1: Alignment stage (Top view).

The theoretical contribution of this work is the development of a mathematical framework for the cooperative landing strategy between an aircraft and a moving ground vehicle. A feedback controller is proposed to synchronize both vehicles, reaching the same position at a defined distance. The stability analysis of the closed-loop system is guaranteed using Lyapunov function theory. It is worth noticing that even though we are using a feedback linearization approach which is well known the application of this technique to deal with the rendezvous problem, is not straightforward. For instance, the control strategy involves the inverse of a matrix and we have found a domain of attraction such that the inverse always exists.

The manuscript is organized as follows: the problem statement and preliminaries are given in Section 2. The equations involved in the system model are described in Section 3. The state feedback control using Lie derivatives is developed in Section 4. The Lyapunov stability analysis is presented in Section 5. Numerical simulation results validate the proposed strategy in Section 6. Finally, concluding remarks and future research directions are presented in Section 7.

2 Problem statement and preliminaries

The objective of the control strategy is to land a fixed-wing drone on a moving ground target. This control scheme is divided into three stages: the alignment of the ground vehicle to the X axis, the alignment of the aerial vehicle to the $X-Z$ plane, and the landing stage. In the landing stage, both vehicles are synchronized to reach the same position at a defined distance.

Figure 2 shows the airplane attitude. χ is the flight course angle, which performs the lateral motion. γ is the flight path angle which modifies the altitude.

The kinematic equations for the ground vehicle are described as in [29],

$$\dot{x}_g = v_g \cos\chi_g \tag{1}$$
$$\dot{y}_g = v_g \sin\chi_g \tag{2}$$
$$\dot{\chi}_g = u_{\chi_g} \tag{3}$$
$$\dot{v}_g = u_g \tag{4}$$

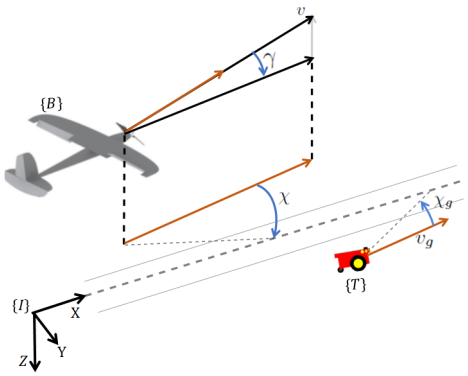

Fig. 2: Representation of the flight path angle γ and the flight course angle χ_g.

where the ground vehicle's position is denoted by (x_g, y_g), v_g is the speed, χ_g is the course angle, and the control inputs are given by u_{χ_g} and u_g.

The lateral motion of the ground vehicle is stabilized to track the X axis, thus, the desired lateral displacement is $y_g^d = 0$.

Therefore, we propose a Lyapunov function candidate as

$$V_1 = \frac{1}{2}\left(y_g + \dot{y}_g\right)^2 \tag{5}$$

Differentiating the above and using (2) and (3),

$$\begin{aligned}\dot{V}_1 &= \left(y_g + \dot{y}_g\right)\left(\dot{y}_g + \ddot{y}_g\right)\\ &= \left(y_g + \dot{y}_g\right)\left(v_g \sin\chi_g + \dot{v}_g \sin\chi_g + v_g u_{\chi_g} \cos\chi_g\right)\end{aligned} \tag{6}$$

Considering the following control law

$$u_{\chi_g} = \frac{1}{v_g \cos\chi_g}\left[-v_g \sin\chi_g - \dot{v}_g \sin\chi_g - k_1\left(y_g + \dot{y}_g\right)\right] \tag{7}$$

Then, introducing (7) into (6), it yields

$$\dot{V}_1 = -k_1\left(y_g + \dot{y}_g\right)^2 \tag{8}$$

where k_1 is a positive constant.

Therefore, y_g and $\dot{y}_g$ tend to zero, then $\chi_g \to 0$. This implies that the ground vehicle dynamics can be reduced to

$$\dot{x}_g = v_g \tag{9}$$
$$\dot{v}_g = u_g \tag{10}$$

The fixed-wing drone equations of the kinematic model are described as in [30]:

$$\dot{x} = v \cos\chi \cos\gamma \tag{11}$$
$$\dot{y} = v \sin\chi \cos\gamma \tag{12}$$
$$\dot{z} = -v \sin\gamma \tag{13}$$
$$\dot{\chi} = u_\chi \tag{14}$$
$$\dot{\gamma} = u_\gamma \tag{15}$$

where the airspeed v is assumed to be constant.

In order to align the aircraft to the $X-Z$ plane, we define the desired lateral displacement as $y^d = 0$.

Assume a Lyapunov function candidate as

$$V_2 = \frac{1}{2}(y+\dot{y})^2 \tag{16}$$

Differentiating the above expression

$$\dot{V}_2 = (y+\dot{y})(\dot{y}+\ddot{y}) \tag{17}$$

$$= (y+\dot{y})(v\sin\chi\cos\gamma + v[\dot{\chi}\cos\chi\cos\gamma - \dot{\gamma}\sin\chi\sin\gamma]) \tag{18}$$

Consider the following control law

$$u_\chi = \frac{-v\sin\chi\cos\gamma + \dot{\gamma}\sin\chi\sin\gamma - k_1(y+\dot{y})}{v\cos\chi\cos\gamma} \tag{19}$$

Then, substituting (19) into (18), yields

$$\dot{V}_2 = -k_2(y+\dot{y})^2 \tag{20}$$

where k_2 is a positive constant.
From (16) and (20), it follows that $y, \dot{y} \to 0$.
In this flight stage, we assume that the aircraft's altitude is constant, that is, $\gamma = 0$. Thus, from (12), it follows $\chi \to 0$. Therefore, system (11)-(15) can be simplified as follows

$$\dot{x} = v\cos\gamma \tag{21}$$

$$\dot{z} = -v\sin\gamma \tag{22}$$

$$\dot{\gamma} = u_\gamma \tag{23}$$

Once both vehicles are aligned in the X axis, the landing strategy can be performed. This strategy is studied in the $X-Z$ plane.

Therefore, a dynamic landing trajectory is designed to lead the aircraft towards the target position.

The desired trajectory performs a descending slope, reducing its distance with respect to the target displacement, keeping a η constant angle. The follower reaches the target's position after the target navigates a defined distance denoted by d_T, see Figure 3. The d_T path parameter represents the target path length, that is, $x_g = d_T$. The initial positions of the follower and target vehicles are denoted by $(x(0), z(0))$ and $(x_g(0), 0)$, respectively.

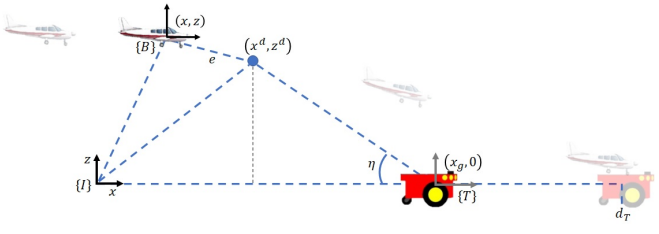

Fig. 3: Dynamic path following control scheme.

The desired trajectory is defined as:

$$x^d = x_g - (d_T - x_g)\cos\eta \tag{24}$$

$$z^d = (d_T - x_g)\sin\eta \tag{25}$$

Notice from the above that

$$\tan\eta = \frac{z^d}{x_g - x^d}. \tag{26}$$

Figure 4 shows the desired trajectory behavior (red line) with respect to the moving target in a straight line (blue line), keeping the η angle constant. Moreover, the desired position is associated with the target's position by the use of reference circles. We can notice that the distance between the desired point and the target's position is reduced.

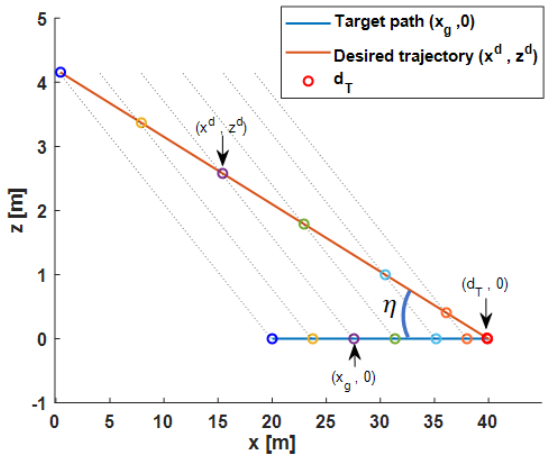

Fig. 4: Study of the desired trajectory behavior, to reach the target position.

3 Longitudinal motion kinematic equations

The system model is rewritten considering the longitudinal equations of the kinematic model and the path parameter dynamics as follows:

$$\dot{\zeta} = f(\zeta) + gu \tag{27}$$

where $\zeta = [x,\ z,\ \gamma,\ x_g,\ \dot{x}_g]^T$ represents the state vector of the system,

$$f(\zeta) = \begin{bmatrix} v\cos\gamma \\ -v\sin\gamma \\ 0 \\ \dot{x}_g \\ 0 \end{bmatrix}, \qquad g = \begin{bmatrix} 0 & 0 \\ 0 & 0 \\ 1 & 0 \\ 0 & 0 \\ 0 & 1 \end{bmatrix}, \tag{28}$$

and the control input vector can be defined as

$$u = [u_\gamma,\ u_g]^T. \tag{29}$$

We have considered the aircraft's speed constant only to simplify the analysis. It turns out that by controlling the speed of the ground vehicle and the navigation angle of the aircraft the landing maneuver can be achieved.

4 State feedback control law

The dynamic path following error is expressed by:

$$e = \begin{bmatrix} e_x \\ e_z \end{bmatrix} = \begin{bmatrix} x \\ z \end{bmatrix} - \begin{bmatrix} x_g - (d_T - x_g)\cos(\eta) \\ (d_T - x_g)\sin(\eta) \end{bmatrix} \tag{30}$$

The derivative of the error is given as:

$$\dot{e} = \frac{\partial e}{\partial \zeta}\dot{\zeta} \tag{31}$$

introducing (27) into (31), it follows that

$$\dot{e} = \frac{\partial e}{\partial \zeta}\left(f(\zeta) + gu\right) \tag{32}$$

the expressions $L_f e = \frac{\partial e}{\partial \zeta} f(\zeta)$ and $L_g e = \frac{\partial e}{\partial \zeta} g$ are the Lie derivatives. Rewriting (32), it yields

$$\dot{e} = L_f e + L_g e u \tag{33}$$

Developing the Lie derivatives:

$$L_f e = \underbrace{\begin{bmatrix} 1 & 0 & 0 & -(1+\cos\eta) & 0 \\ 0 & 1 & 0 & \sin\eta & 0 \end{bmatrix}}_{\frac{\partial e}{\partial \zeta}} \underbrace{\begin{bmatrix} v\cos\gamma \\ -v\sin\gamma \\ 0 \\ \dot{x}_g \\ 0 \end{bmatrix}}_{f(\zeta)}$$

$$= \begin{bmatrix} v\cos\gamma - \dot{x}_g\left(1+\cos\eta\right) \\ -v\sin\gamma + \dot{x}_g\sin\eta \end{bmatrix} \tag{34}$$

Note that $L_g e = \bar{0}_{2\times 2}$. Therefore, the derivative of the error is described as:

$$\dot{e} = L_f e \tag{35}$$

Now, $\ddot{e}$ can be expressed as follows

$$\begin{aligned} \ddot{e} &= \frac{\partial L_f e}{\partial \zeta}\dot{\zeta} \\ &= \frac{\partial L_f e}{\partial \zeta}\left(f(\zeta) + gu\right) \\ &= L_f^2 e + L_g L_f e u \end{aligned} \tag{36}$$

where $L_f^2 e = \frac{\partial (L_f e)}{\partial \zeta} f(\zeta)$ and $L_g e = \frac{\partial (L_f e)}{\partial \zeta} g$.

Developing the Lie derivatives of (36), we obtain that the vector $L_f^2 e = \bar{0}_{2\times 1}$. Therefore, the second derivative of the error is expressed as:

$$\ddot{e} = L_g L_f e u \tag{37}$$

where

$$L_g L_f e = \underbrace{\begin{bmatrix} 0 & 0 & -v\sin\gamma & 0 & -(1+\cos\eta) \\ 0 & 0 & -v\cos\gamma & 0 & \sin\eta \end{bmatrix}}_{\frac{\partial (L_f e)}{\partial \zeta}} \underbrace{\begin{bmatrix} 0 & 0 \\ 0 & 0 \\ 1 & 0 \\ 0 & 0 \\ 0 & 1 \end{bmatrix}}_{g}$$

$$= \begin{bmatrix} -v\sin\gamma & -(1+\cos\eta) \\ -v\cos\gamma & \sin\eta \end{bmatrix} \tag{38}$$

From (37), the system can be stabilized using the following controller:

$$u = \left(L_g L_f e\right)^{-1}\left[-c_1 e - c_2 \dot{e}\right] \tag{39}$$

where $c_1 > 0$ and $c_2 > 0$ are positive constants.

This control strategy assumes the speed of the ground vehicle is always positive, i.e. $\dot{x}_g > 0$, and has a lower bound that is sufficiently large to avoid numerical condition issues.

Now, introducing the control law (39) into (37) leads to

$$\ddot{e} = -c_1 e - c_2 \dot{e} \tag{40}$$

5 Stability analysis

The Lyapunov analysis will be carried out with respect to the error components of the X axis, and the same process will be applied with the error components of the Z axis. Therefore, defining

$$\xi_x = \left[e_x,\ \dot{e}_x\right]^T \tag{41}$$

and considering the components of the X axis of (30) and (40), it can be expressed as:

$$\dot{\xi}_x = \begin{bmatrix} \dot{e}_x \\ \ddot{e}_x \end{bmatrix} = A\xi_x = \underbrace{\begin{bmatrix} 0 & 1 \\ -c_1 & -c_2 \end{bmatrix}}_{A} \xi_x \tag{42}$$

Computing the determinant of (42), it follows

$$\begin{aligned} det(\lambda I - A) &= det\left(\begin{bmatrix} \lambda & -1 \\ c_1 & \lambda + c_2 \end{bmatrix}\right) \\ &= \lambda^2 + c_2\lambda + c_1 \end{aligned} \tag{43}$$

From (43), it follows that the eigenvalues of A are negative, that is, A is Hurwitz. The closed loop system corresponding to the X-axis is stable.

Therefore, for any Q positive definite matrix, there exists a P symmetric positive definite matrix such that the following Lyapunov equation holds

$$A^T P + PA = -Q \tag{44}$$

Let us propose the following Q matrix

$$Q = \begin{bmatrix} 2c_1c_2 & 0 \\ 0 & 2c_2 \end{bmatrix} \tag{45}$$

The following P matrix is determined by solving (44),

$$P = \begin{bmatrix} 2c_1 + c_2^2 & c_2 \\ c_2 & 2 \end{bmatrix} \tag{46}$$

Therefore, we propose a positive function:

$$V_3 = \xi_x^T P \xi_x \tag{47}$$

Differentiating the above equation

$$\dot{V}_3 = \dot{\xi}_x^T P \xi_x + \xi_x^T P \dot{\xi}_x \tag{48}$$

Introducing (42) into (48), it yields

$$\begin{aligned}\dot{V}_3 &= \xi_x^T A^T P \xi_x + \xi_x P A \xi_x \\ &= \xi_x^T \left(A^T P + P A\right) \xi_x \end{aligned} \tag{49}$$

substituting (44) into (49):

$$\dot{V}_3 = -\xi_x^T Q \xi_x \tag{50}$$

We have then proved the following Lemma,

Lemma 1 *The error dynamical system* (42) *having* ξ_x *as state* (41) *has a Lyapunov function as in* (47) *whose derivative satisfies* (50). *Therefore, the system* (42) *is exponentially stable i.e;* ξ_x *converges to* 0 *exponentially fast.*

Now, analyzing the case with respect to the error in the Z axis, e_z. Defining,

$$\xi_z = [e_z,\ \dot{e}_z]^T \tag{51}$$

and considering the components of the Z axis of (30) and (40), it can be expressed as:

$$\dot{\xi}_z = \begin{bmatrix} \dot{e}_z \\ \ddot{e}_z \end{bmatrix} = A\xi_z = \underbrace{\begin{bmatrix} 0 & 1 \\ -c_1 & -c_2 \end{bmatrix}}_{A} \xi_z \tag{52}$$

A positive function is proposed as follows:

$$V_4 = \xi_z^T P \xi_z \tag{53}$$

Differentiating the above equation

$$\dot{V}_4 = \dot{\xi}_z^T P \xi_z + \xi_z^T P \dot{\xi}_z \tag{54}$$

Introducing (42) into (54), it yields

$$\begin{aligned}\dot{V}_4 &= \xi_z^T A^T P \xi_z + \xi_z P A \xi_z \\ &= \xi_z^T \left(A^T P + P A\right) \xi_z \end{aligned} \tag{55}$$

substituting (44) into (55):

$$\dot{V}_4 = -\xi_z^T Q \xi_z \tag{56}$$

We have then proved the following Lemma,

Lemma 2 *The error dynamical system* (52) *having* ξ_z *as state* (51) *has a Lyapunov function as in* (53) *whose derivative satisfies* (56). *Therefore, the system* (52) *is exponentially stable i.e;* ξ_z *converges to* 0 *exponentially fast.*

Using the Lyapunov stability theory we conclude that the closed loop system is stable.

In the previous section, it was concluded that the system is stable. However, it is necessary to guarantee that the inverse matrix of $L_g L_f e$ exists.

$$L_g L_f e = \begin{bmatrix} -v\sin\gamma & -(1+\cos\eta) \\ -v\cos\gamma & \sin\eta \end{bmatrix} \tag{57}$$

and its determinant is given as

$$det\left(L_g L_f e\right) = -v\sin\gamma\sin\eta - v\cos\gamma\left(1+\cos\eta\right) \tag{58}$$

Differentiating (30) and introducing (21) and (22) leads to,

$$\dot{e}_x = \dot{x} - \dot{x}_g\left(1+\cos\eta\right) \tag{59}$$

$$\dot{e}_z = \dot{z} + \dot{x}_g \sin\eta \tag{60}$$

thus, the above can be rewritten as

$$\frac{\dot{x} - \dot{e}_x}{\dot{x}_g} = (1+\cos\eta) \tag{61}$$

$$\frac{-\dot{z} + \dot{e}_z}{\dot{x}_g} = \sin\eta \tag{62}$$

Then, introducing (21) and (22) into (61) and (62) respectively it follows:

$$\frac{v\cos\gamma - \dot{e}_x}{\dot{x}_g} = (1+\cos\eta) \tag{63}$$

$$\frac{v\sin\gamma + \dot{e}_z}{\dot{x}_g} = \sin\eta \tag{64}$$

Now, introducing (63) and (64) into (57), leads to

$$L_g L_f e = \begin{bmatrix} -v\sin\gamma & \frac{-v\cos\gamma + \dot{e}_x}{\dot{x}_g} \\ -v\cos\gamma & \frac{v\sin\gamma + \dot{e}_z}{\dot{x}_g} \end{bmatrix} \tag{65}$$

Computing the determinant of the above expression, and grouping terms, yields

$$det\left(L_g L_f e\right) = -\frac{v^2}{\dot{x}_g} - \frac{v}{\dot{x}_g}\left(\sin\gamma\dot{e}_z - \cos\gamma\dot{e}_x\right) \tag{66}$$

From (41), (47) and (50) it follows that

$$\begin{aligned}\lambda_{min}\left(P\right)\dot{e}_x^2 &\leq \lambda_{min}\left(P\right)\left(e_x^2 + \dot{e}_x^2\right) \\ &\leq \lambda_{min}\left(P\right)||\xi_x||^2 \\ &\leq \xi_x^T P \xi_x = V_3 \\ &\leq V_3(0) \end{aligned} \tag{67}$$

Let us assume that the initial conditions satisfy

$$V_3(0) = v^2 k^2 \frac{\lambda_{min}(P)}{4} \tag{68}$$

Introducing the above into (67) yields

$$|\dot{e}_x| \leq \frac{vk}{2} \tag{69}$$

From (51), (53), and (55), it follows that

$$\begin{aligned}\lambda_{min}(P)\,\dot{e}_z^2 &\leq \lambda_{min}(P)\left(e_z^2+\dot{e}_z^2\right)\\ &\leq \lambda_{min}(P)\,||\xi_z||^2\\ &\leq \xi_z^T P\xi_z = V_4\\ &\leq V_4(0)\end{aligned} \tag{70}$$

Let us assume that the initial conditions satisfy

$$V_4(0) = v^2k^2\frac{\lambda_{min}(P)}{4} \tag{71}$$

Introducing the above into (70) yields

$$|\dot{e}_z| \leq \frac{vk}{2} \tag{72}$$

From (69) and (72) it follows

$$|\dot{e}_x| + |\dot{e}_z| \leq vk \tag{73}$$

Therefore, from (66) and (73), it follows

$$|det\,(L_gL_fe)| \geq \left|-\frac{v^2}{\dot{x}_g}\right| - \left|\frac{v}{\dot{x}_g}\right|(|\sin\gamma\dot{e}_z - \cos\gamma\dot{e}_x|) \tag{74}$$

$$\geq \left|\frac{v^2}{\dot{x}_g}\right| - \left|\frac{v}{\dot{x}_g}\right|(|\dot{e}_z| + |\dot{e}_x|) \tag{75}$$

$$\geq \left|\frac{v^2}{\dot{x}_g}\right| - \left|\frac{v}{\dot{x}_g}\right|(vk) \tag{76}$$

$$\geq \left|\frac{v^2}{\dot{x}_g}\right| - \left|\frac{v^2}{\dot{x}_g}\right|k = \left|\frac{v^2}{\dot{x}_g}\right|(1-k) \tag{77}$$

A lower bound for (66) should be obtained to guarantee that (65) is a nonsingular matrix. Notice from (66) that if the derivatives of the errors are small enough, then the determinant will be different from zero. In other words, if $(|\dot{e}_x| + |\dot{e}_z|) < vk$, then the RHS of (66) will be different from zero for some $k < 1$. To obtain such an upper bound we assume that $V_3(0)$ satisfies (68). This allows us to conclude that $|\dot{e}_x|$ satisfies (69). Similarly, we assume that $V_4(0)$ satisfies (71) and thus the upper bound for $|\dot{e}_z|$ is given in (72). Adding (69) and (72) leads to (73). Finally, introducing (73) into (66) gives (77) which proves that the determinant is different from zero for $k < 1$. This result is stated in lemma 3.

Lemma 3 *The determinant of* (38) *will be different from zero for* $k < 1$*, and the domain of attraction is given by* (67), (68), (70) *and* (71).

The stability of the control strategy is guaranteed only if the initial conditions belong to a given set in the attraction domain. Otherwise, several maneuvers could be performed so that the system is driven to the attraction domain, this could be treated in a new research study.

6 Numerical simulation results

A cooperative strategy is simulated to validate the control design based on the Lie derivatives, which focuses on landing a fixed-wing drone on a moving ground vehicle. The first stage of this strategy consists of aligning both vehicles in the $X-Z$ plane. Then, the landing stage will apply once the ground vehicle reaches position P_i, which is defined as $P_i = (0, 0, 0)$. The landing stage focuses on guiding the aircraft through a desired trajectory and controlling the ground vehicle's speed.

The parameters d_T and η will be used to calculate the desired trajectory for the UAV. These parameters are chosen as $d_T = 20$ meters and $\eta = 12°$.

In the alignment stage, the ground vehicle is aligned to the X axis while it navigates with a constant speed of $v_g = 1.5$ m/s. Besides, the aerial vehicle is aligned to the $X-Z$ plane, keeping a desired altitude. The drone's references were obtained solving (24) and (25) for P_i, that is, $(x^d, y^d, z^d) = (-19.5, 0, 4.15)$.

The landing control strategy synchronizes both vehicles to reach a predefined position at a given distance d_T. The ground vehicle's speed is controlled by taking into account the aircraft's position. The aircraft modifies its flight path angle to track a trajectory keeping a constant airspeed of 4 m/s. Therefore, the UAV should be on the dynamic landing trajectory at any point in time depending on where the ground vehicle is located. The desired point is calculated from (24) and (25) given the ground vehicle location and the desired path parameters. The speed of the ground vehicle is controlled to reach the distance d_T at the same time as the aircraft.

In addition, wind disturbances are involved as variations in aircraft velocities, using a wind model as in [31]. The wind speed changes in a range of $[0.8\,,\,-0.72]$ m/s.

The simulation result of the cooperative control strategy for landing a fixed-wing drone on a ground vehicle in 3D space is shown in Figure 5. The target path is given by a blue line, the desired trajectory is represented by a red dash line, and the follower path is given by a purple line. We observe that the vehicles align with the X-axis. External disturbances on the three axes are applied to the aircraft to study the control performance. Once the ground vehicle reaches the X axis at position P_i, then, the landing stage starts to be performed. Figure 5 shows as the drone performs a descending flight to reach the target position.

The performance of the alignment stage is shown in Figure 6. Both vehicles tend to converge on the X-axis until completing the mission. The wind disturbances are not involved in the ground vehicle motion.

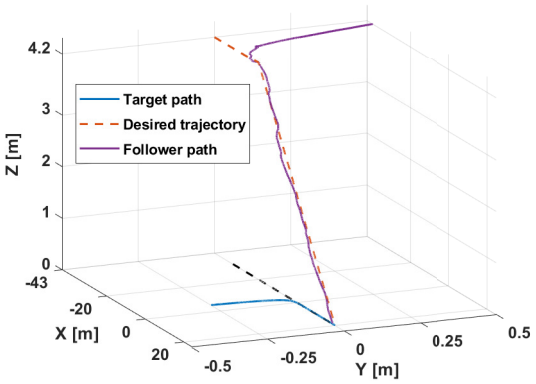

Fig. 5: Cooperative control strategy for landing a fixed-wing drone on a moving ground vehicle: alignment stage and landing stage (3D view).

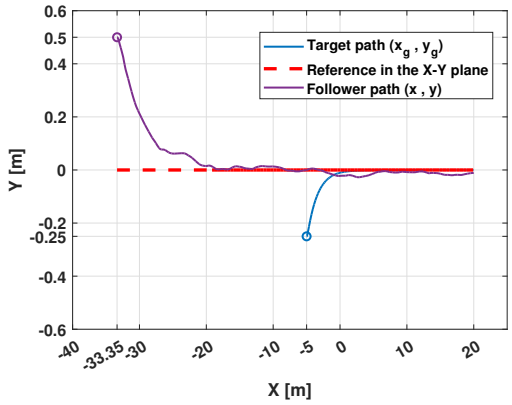

Fig. 6: Alignment stage in the $X-Y$ plane (Top view).

The simulation result of the control strategy in the $X-Z$ plane is shown in Figure 7. The strategy is divided into two stages: the alignment stage is denoted by AS, and the landing stage is represented by LS.

In the alignment stage, the altitude reference is constant to guide the aircraft close to the desired landing trajectory, which starts to be tracked from the position $x=-20$ m. Besides, the trajectory maintains the angle η throughout the movement of the target vehicle.

The tracking of the descending slope is executed by the drone, which is affected by wind disturbances. However, the aircraft follows the desired trajectory. Analyzing the convergence distance d_T, in the picture zoom, observe that there exists a minimum distance between the positions of the vehicles.

Notice from (24) and (25) than when $(d_T - x_g)$ converges to 0, x^d converges to x_g and z^d converges to 0.

Considering the alignment stage, the ground vehicle is aligned to the X axis by the modification of the course angle χ_g. The course angle is controlled by the u_{χ_g} control input, see Figure 8.

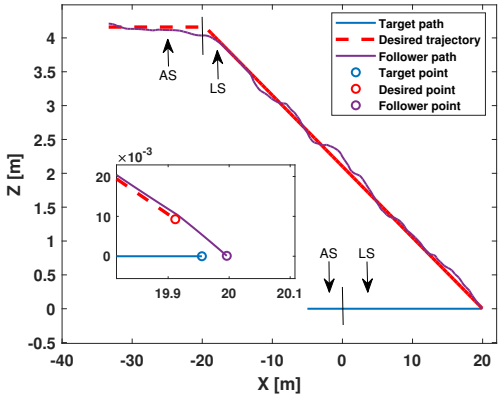

Fig. 7: The target and fixed-wing drone reach the rendez-vous point.

The aircraft is aligned to the $X-Z$ plane by the u_χ control input, which modifies the course flight angle χ, see Figure 9. In addition, the flight path angle γ is affected by the disturbances. Thus, the u_γ control input is adjusted to modify the flight path angle in order to track the trajectory. The behavior of γ and u_γ are shown in Figure 10.

Figure 11 presents the evolution of $\dot{x}_g$ and the control input u_g. The control input u_g allows the synchronization of the ground vehicle to reach the distance d_T at the same time as the fixed wing drone.

Based on the stabilization of the flight path angle by the u_γ control input, the tracking errors approximated to zero along the dynamic path following strategy, as shown in Figure 12. Moreover, the derivatives of the tracking errors e_x and e_z satisfy condition (73). It means that the addition of the absolute value of the error derivatives is less than the airspeed of the fixed-wing drone ($|\dot{e}_x| + |\dot{e}_z| \leq 4\, m/s$), see Figure 13.

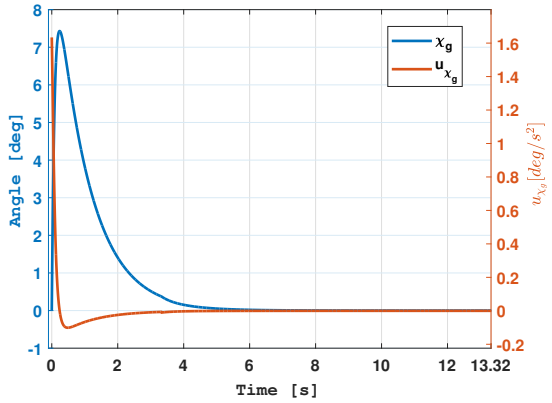

Fig. 8: Alignment of the ground vehicle to the X axis by the modification of χ_g.

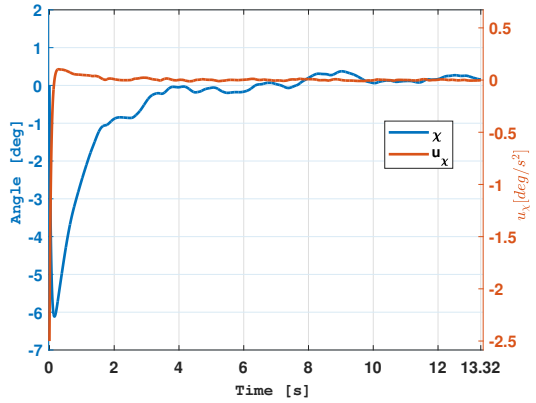

Fig. 9: Performance of χ_g and u_{χ_g} to align the aircraft in the $X-Z$ plane.

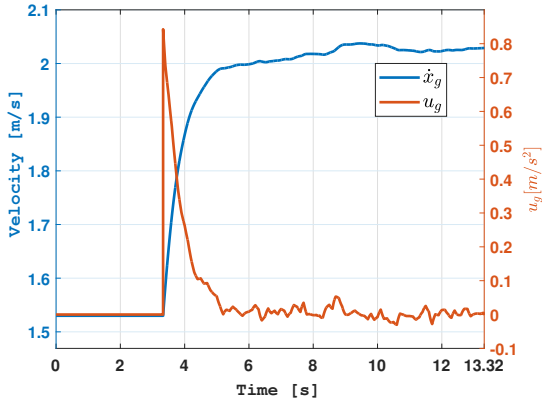

Fig. 11: Behavior of the u_g control to modify $\dot{x}_g$.

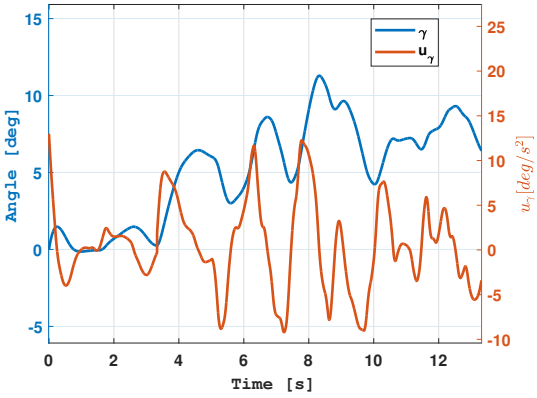

Fig. 10: Modification of the flight path angle and its control input for tracking.

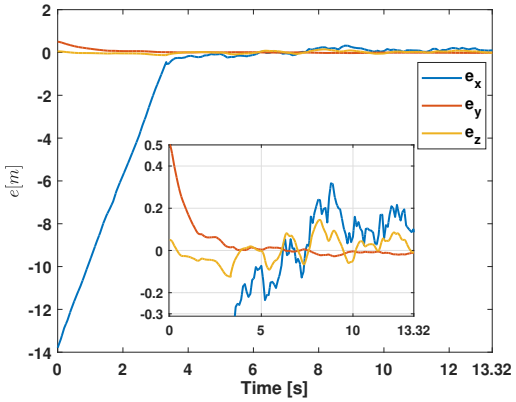

Fig. 12: Position errors converge to zero in a tridimensional space.

7 Conclusions

In this paper, a cooperative control strategy for landing a fixed-wing drone on a moving ground vehicle was presented. The strategy focused on the alignment of both vehicles in the $X-Z$ plane, and then, the synchronization of both vehicle to reach the same position in a desired distance. The descending trajectory was proposed to guide the aerial vehicle towards the rendezvous point. The target position x_g was used as the path parameter. The system model was given by the kinematic model of the fixed-wing drone and the ground vehicle. We proposed a state feedback control law, which is expressed in Lie derivatives with respect to the tracking error. In addition, the control law involves the inverse of a matrix, however we have found an attraction domain where the inverse exists. Finally, it has been proved that the closed loop system is stable using the Lyapunov stability theory. Numerical simulations illustrated the good performance of the proposed strategy.

Future work

Future work includes adding a flight stage to develop a trajectory based on the position of the target vehicle before carrying out the landing strategy with a smoother maneuver. Moreover, the controller should have robustness properties to attenuate the undesired effects of external disturbances when the fixed-wing vehicle navigates towards the target. A practical validation of the strategy is also considered as future work.

Acknowledgment

This paper was supported by the RPV project - UTC foundation and the Mexican National Council of Science and Technology - CONACyT.

Declarations

Funding:

Our research work has been financed by the RPV project - UTC foundation and the Mexican National Council of Science and Technology - CONACyT.

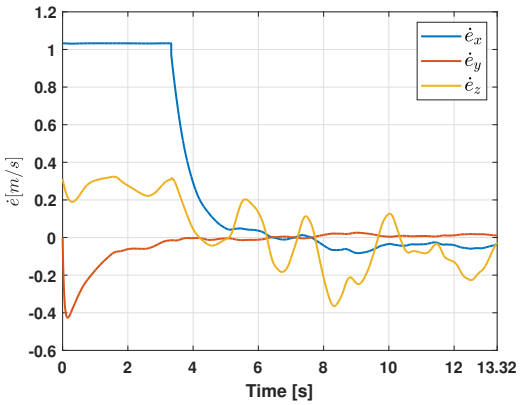

Fig. 13: Derivatives of the tracking error satisfy condition (73) and converge to zero.

Conflict of interest:

The authors have no financial or proprietary interests in any material discussed in this article.

Ethics approval:

The submitted work is original and it has not been submitted to other journals.

Consent to participate:

All authors approve their participation.

Consent for publication:

All authors approve the publication of the scientific article.

Availability of data and materials:

Not applicable.

Code availability:

Not applicable.

Authors' contributions:

All authors contributed to the study conception and design. Analysis, investigation and methodology were performed by Rogelio Lozano, Armando Alatorre and Pedro Castillo. The first draft of the manuscript was written by Armando Alatorre and all authors commented on previous versions of the manuscript. All authors read and approved the final manuscript.

References

1. S. Huh and D. H. Shim, "A vision-based landing system for small unmanned aerial vehicles using an airbag", *Control Engineering Practice*, 2010, vol. 18, no. 7, pp. 812-823.
2. D. Zhang,& X. Wang. "Autonomous landing control of fixed-wing uavs: from theory to field experiment". *Journal of Intelligent & Robotic Systems*, 2017, 88(2-4), 619.
3. M. Ruchanurucks, P. Rakprayoon, & S. Kongkaew. "Automatic Landing Assist System Using IMU+ P n P for Robust Positioning of Fixed-Wing UAVs". *Journal of Intelligent & Robotic Systems*, 2018, 90(1), 189-199.
4. O. A. Yakimenko, I. I. Kaminer, W. J. Lentz, & P. A. Ghyzel. "Unmanned aircraft navigation for shipboard landing using infrared vision". *IEEE Transactions on Aerospace and Electronic Systems*, 2002, 38(4), 1181-1200.
5. S. Mathisen, K. Gryte, S. Gros, & T. A. Johansen. "Precision Deep-Stall Landing of Fixed-Wing UAVs Using Nonlinear Model Predictive Control". *Journal of Intelligent & Robotic Systems*, 2021, 101(1), 1-15.
6. B. Barber, T McLain & B. Edwards. "Vision-based landing of fixed-wing miniature air vehicles". *Journal of Aerospace Computing, Information, and Communication*, 2009, 6(3), 207-226.
7. T. Muskardin, G. Balmer, L. Persson, S. Wlach, M. Laiacker, A. Ollero & K. Kondak. "A novel landing system to increase payload capacity and operational availability of high altitude long endurance UAVs". *Journal of Intelligent & Robotic Systems*, 2017, 88(2), 597-618.
8. L. Persson, T. Muskardin, & B. Wahlberg. (2017, December). "Cooperative rendezvous of ground vehicle and aerial vehicle using model predictive control". *56th Annual Conference on Decision and Control (CDC)*, 2017, (pp. 2819-2824). IEEE.
9. T. Oliveira, & P. Encarnacao, "Ground target tracking control system for unmanned aerial vehicles". *Journal of Intelligent & Robotic Systems* 2013; 69(1), 373-387.
10. T. Oliveira, A. P. Aguiar and P. Encarnacao. "Moving Path Following for Unmanned Aerial Vehicles With Applications to Single and Multiple Target Tracking Problems". *IEEE Transactions on Robotics* 2016; 32(5): 1062-1078.
11. T. Oliveira, A. P. Aguiar and P. Encarnacao. "Three dimensional moving path following for fixed-wing unmanned aerial vehicles". *IEEE International Conference on Robotics and Automation (ICRA)* 2017; 2710-2716.
12. Y. Wang, D. Wang, & S. Zhu. "Cooperative moving path following for multiple fixed-wing unmanned aerial vehicles with speed constraints". *Automatica* 2019; 100, 82-89.
13. R. Skjetne, T. I. Fossen, & P. V. Kokotović. "Robust output maneuvering for a class of nonlinear systems". *Automatica*, 40(3), 2004, 373-383.
14. Z. Zheng. "Moving path following control for a surface vessel with error constraint". *Automatica*, 2020, vol 118, pp. 1-7.
15. L. Lapierre, D. Soetanto, & A. Pascoal. "Nonsingular path following control of a unicycle in the presence of parametric modelling uncertainties". *International Journal of Robust and Nonlinear Control: IFAC-Affiliated Journal* 2006; 16(10), 485-503.
16. M. F. Reis, R. P. Jain, A. P. Aguiar and J. B. de Sousa, "Robust Moving Path Following Control for Robotic Vehicles: Theory and Experiments". *IEEE Robotics and Automation Letters* 2019; 4(4): 3192-3199.
17. C. Liu, O. McAree, & W. H. Chen. "Path-following control for small fixed-wing unmanned aerial vehicles under wind disturbances". *International Journal of Robust and Nonlinear Control* 2013;, 23(15):1682-1698.
18. S. Thakar, & A. Ratnoo. "Rendezvous guidance laws for aerial recovery using mothership-cable-drogue system". *IFAC-PapersOnLine* 2016; 49(1): 24-29.

19. J. W. Nichols, L. Sun, R. W. Beard, & T. McLain. "Aerial rendezvous of small unmanned aircraft using a passive towed cable system". *Journal of Guidance, Control, and Dynamics* 2014; 37(4): 1131-1142.
20. H. Oh, S. Kim, H. S. Shin, B. A. White, A. Tsourdos, & C. A. Rabbath. "Rendezvous and standoff target tracking guidance using differential geometry". *Journal of Intelligent & Robotic Systems* 2013; 69(1): 389-405.
21. S. Park. "Rendezvous Guidance on Circular Path for Fixed-Wing UAV". *International Journal of Aeronautical and Space Sciences* 2021; 22(1): 129-139.
22. B. A. White, R. Zbikowski & A. Tsourdos. "Direct intercept guidance using differential geometry concepts". *IEEE Transactions on Aerospace and Electronic Systems* 2007; 43(3): 899-919.
23. B. C. Mitra, & S. Hota. "Optimal Path Generation for Simultaneous Rendezvous of Fixed-Wing UAVs in 3D Dynamic Environments". *AIAA Scitech 2019 Forum* 2019; 1166.
24. C. Hu, Z. Meng, G. Qu, H. S. Shin, & A. Tsourdos. "Distributed cooperative path planning for tracking ground moving target by multiple fixed-wing UAVs via DMPC-GVD in urban environment". *International Journal of Control, Automation and Systems* 2021; 19(2): 823-836.
25. R. Li, Y. Shi, & K. L. Teo. "Coordination arrival control for multi-agent systems". *International Journal of Robust and Nonlinear Control* 2016; 26(7): 1456-1474.
26. A. Tsukerman, M. Weiss, T. Shima, D. Löbl, & F. Holzapfel. "Optimal rendezvous guidance laws with application to civil autonomous aerial refueling". *Journal of Guidance, Control, and Dynamics* 2018; 41(5): 1167-1174.
27. A. Rucco, P. B. Sujit, A. P. Aguiar, J. B. De Sousa, & F. L. Pereira. "Optimal rendezvous trajectory for unmanned aerial-ground vehicles". *IEEE Transactions on Aerospace and Electronic Systems* 2017; 54(2): 834-847.
28. J. Yang, C. Liu, M. Coombes, Y. Yan, & W. Chen. "Optimal path following for small fixed-wing UAVs under wind disturbances". *IEEE Transactions on Control Systems Technology* 2020; 29(3): 996-1008.
29. R. Rajamani, "Vehicle dynamics and control". *Springer Science & Business Media* 2011.
30. R. W. Beard and T. W. McLain, "Small Unmanned Aircraft: Theory and Practice", *Princeton Univ. Press* 2012; 1st ed. Princeton.
31. A. Chapman, A., & M. Mesbahi. "Uav flocking with wind gusts: Adaptive topology and model reduction". *American Control Conference* 2011; pp. 1045-1050. IEEE.